Organic & Biomolecular Chemistry

ROYAL SOCIETY OF CHEMISTRY

PAPER

View Article Online
View Journal | View Issue

Open Access Article. Published on 24 September 2024. Downloaded on 1/21/2026 10:08:25 PM.
This article is licensed under a Creative Commons Attribution-NonCommercial 3.0 Unported Licence.

Check for updates

Cite this: *Org. Biomol. Chem.*, 2024, **22**, 8323

Continuous flow synthesis of the antiviral drug tecovirimat and related sp^3-rich scaffolds†

Arlene Bonner and Marcus Baumann *

Received 21st August 2024,
Accepted 17th September 2024

DOI: 10.1039/d4ob01379d

rsc.li/obc

Herein we report a 2-step continuous flow synthesis of the antiviral drug tecovirimat, which is used for the treatment of monkeypox and smallpox. This work exploits a high-temperature pericyclic cascade process between cycloheptatriene and maleic anhydride generating a key sp^3-rich scaffold, which affords the desired API after further condensation with an acyl hydrazide. Additional investigations of the key intermediate in reactions with different hydrazines revealed the accessibility of different heterocyclic chemotypes, depending on the substitution pattern of the hydrazine used. Ultimately, the streamlined and scalable access to these sp^3-rich scaffolds enables improved access to tecovirimat and structurally related entities with high drug-like character.

Introduction

Recent years have witnessed an increasing demand for chemical motifs that are rich in sp^3-character. The advantages of such scaffolds in modern medicinal chemistry campaigns arise from the potentially improved binding of such motifs in restricted binding pockets, as well as improved solubility. This has led to defining the fraction of sp^3 hybridised carbon atoms as a metric for assessing drug likeness.[1] Classical three-dimensional scaffolds such as norbornenes,[2] adamantanes[3] and cubanes[4] have thus experienced a revival, with new and improved synthetic routes being of high value (Fig. 1).

Whilst symmetrical three-dimensional motifs dominate in most reported drugs due to simpler synthetic access and the absence of stereoisomerism, several studies employ scaffolds that are desymmetrised. Crucially, for these scaffolds to be synthetically viable, they must be easily accessible from readily available starting materials and their preparation must be safe and scalable to multi-gram quantities.

A unique polycyclic scaffold can be found in the antiviral drug tecovirimat which is used in the treatment of monkeypox and smallpox.[5] The synthesis of the carbocyclic fragment relies on a pericyclic cascade process in which cycloheptatriene and maleic anhydride are reacted at elevated temperature. Detailed studies by Leitich and Sprintschnik have confirmed that an initial 6π-electrocyclisation thereby renders the bicyclic diene, which then engages in a thermal Diels–Alder cycloaddition reaction (Scheme 1).[6] Condensation of the resulting anhydride adduct with an acyl hydrazide subsequently affords the desired drug target. Earlier patented routes[7] often describe the use of xylenes as high-boiling solvent to facilitate the initial pericyclic cascade, however, more recent studies[8] show further improvements in terms of *in situ* generation of cycloheptatriene, solvent choice and yields *en route* to kilogram quantities of tecovirimat.

Due to our interest in exploiting continuous flow approaches for the intensification of chemical reactions, as well as the generation of strained ring systems that have potential applications in medicinal chemistry programs,[9] we wished to develop a fast high-temperature flow process towards tecovirimat. This was expected to deliver multigram quantities of the desired cycloadduct in a safe and streamlined manner which would additionally enable subsequent synthetic studies on this intriguing yet underexplored scaffold. In particular, the use of miniaturised flow set-ups was deemed crucial in achieving improved heat and mass transfer whilst mitigating any

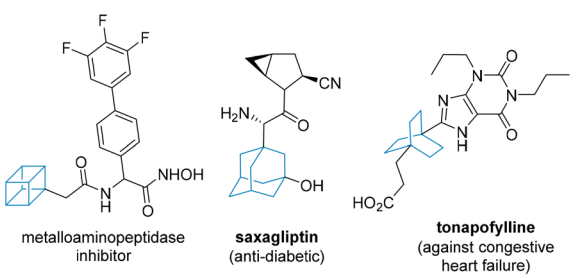

Fig. 1 Representative drugs containing 3D-rich scaffolds.

University College Dublin, School of Chemistry, Science Centre South, D04 N2E5 Dublin, Ireland. E-mail: marcus.baumann@ucd.ie

† Electronic supplementary information (ESI) available: Experimental procedures and ^{1}H, ^{19}F and ^{13}C-NMR spectra for all reported compounds. CCDC 2378696 and 2378697. For ESI and crystallographic data in CIF or other electronic format see DOI: https://doi.org/10.1039/d4ob01379d

Open Access Article. Published on 24 September 2024. Downloaded on 1/21/2026 10:08:25 PM.
This article is licensed under a Creative Commons Attribution-NonCommercial 3.0 Unported Licence.

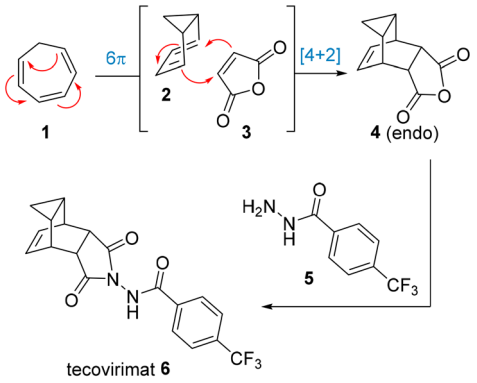

Scheme 1 Structure of tecovirimat and its synthesis in batch mode.

safety concerns as only small amounts of material are within the contained flow system at any given time.[10] As reported previously, these advantages are crucial in the exploitation of continuous flow technology for the generation of active pharmaceutical ingredients (APIs),[11] which oftentimes includes reaction telescoping,[12] inline analysis[13] and inline purification strategies.[14]

Results and discussion

We initiated our study towards scaffold **4** using commercially available cycloheptatriene in combination with maleic anhydride. When replicating the reported batch conditions which entailed longer reaction times (3–12 hours)[7,8,15] in refluxing xylene (b. p. 139 °C), discolouration of the reaction mixture was observed over time indicating thermal degradation. However, shortening the reaction time to 1 hour afforded scaffold **4** in high yield (83%, entry 1), which is comparable to previous reports.[7j] Next, we investigated suitable replacements for xylene as maleic anhydride is not sufficiently soluble in this solvent and its evaporation is time consuming. While toluene was initially investigated for the flow process (89%, 145 °C, t_{Res} 30 min, 0.15 M, 4 bar BPR), its non-polar nature restricts solubility of maleic anhydride and consequently, lowers reaction throughput. Thus, acetonitrile (b. p. 83 °C) was favoured as it is more polar and can be superheated above its atmospheric boiling point using a back-pressure regulator (BPR) in flow. A trial reaction in continuous flow mode rendered the desired product in comparable yield (85%, t_{Res} 45 min) under high temperature/high pressure conditions (entry 2, 145 °C, 8 bar BPR). Encouraged by this improvement we wished to evaluate whether an additional temperature increase would accelerate this pericyclic cascade further. As the PFA tubing (perfluoroalkoxy) starts to soften above 150 °C, we opted to use a batch microwave reactor in this instance which pleasingly gave near quantitative conversion in only 15 min reaction time at 169 °C (toluene, entry 3). This result was replicated on 25 mmol scale, giving the desired product in excellent yield with a productivity of 18.6 g h^{-1} (98 mmol h^{-1}, entry 4). The superiority of the microwave process can be demonstrated by its higher space–time-yield of 0.75 g mL^{-1} h^{-1} of scaffold **4**, in comparison to those of batch and flow (0.16 g mL^{-1} h^{-1} and 0.22 g mL^{-1} h^{-1} respectively). Pleasingly, multigram quantities of **4** were found to be bench stable for months at ambient conditions (Table 1).

Being able to rapidly generate gram quantities of **4** in both batch (MW) and flow mode, we next investigated the flow synthesis of tecovirimat by condensing the commercially available acyl hydrazide **5** with scaffold **4**. For this step ethanol was favoured as a polar, protic solvent and solvent superheating using a BPR was again envisioned to accelerate the desired transformation.

As shown in Table 2, initial trials at 110–130 °C in ethanol in the presence of small amounts of DIPEA gave tecovirimat in up to 85% yield with small amounts of the acyl hydrazide remaining (entries 1–3). Extending the reaction time from 15 to 20 minutes gave a lower yield due to competing side reactions (entry 4). A similar outcome was observed when increasing the temperature to 125 °C (entry 5). Doubling the reaction concentration from 50 mM to 100 mM gave near identical results (entry 6 *vs.* 2), however, the limited solubility of **4** in ethanol did preclude further increasing the concentration. Lastly, a gram-scale experiment was conducted (entry 7) which afforded tecovirimat in 86% isolated yield after hot recrystallisation from a mixture of ethanol/water (5 : 1). This equates to a throughput of 3.3 mmol h^{-1} (*ca.* 1.3 g h^{-1}) representing a highly efficient continuous synthesis of tecovirimat in a total residence time of 1 hour and an overall yield of 84%. The telescoping of these two steps in an acetonitrile/ethanol mixed solvent system did only give a modest yield of tecovirimat (30% overall yield, unoptimised process).

Having a achieved a robust 2-step flow synthesis for the antiviral API tecovirimat, our next target concerned the study of scaffold **4** as a building block towards related entities. Previous studies by Efremova and coworkers[16] had already established that the steric hinderance around the alkene in **4** prevents its reaction in dipolar cycloadditions, which directed our attention to the alternative anhydride functionality.

Table 1 Reaction optimisation for pericyclic cascade process

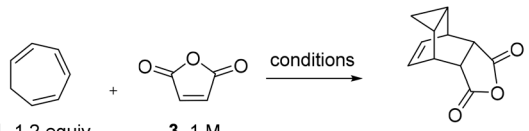

1, 1.2 equiv + **3**, 1 M → **4**, 83-98% (endo)

Entry	Reaction mode	Solvent	Temperature and time	Yield[a] of **4**	Space-time-yield
1	Batch	Xylene	139 °C, 1 h	83%[b]	0.16 g mL^{-1} h^{-1}
2	Flow	MeCN	145 °C, 45 min	85%[c]	0.22 g mL^{-1} h^{-1}
3	MW	Toluene	169 °C, 15 min	98%	0.75 g mL^{-1} h^{-1}
4	MW	Toluene	169 °C, 15 min	98%[b]	0.75 g mL^{-1} h^{-1}

[a] Isolated yield. [b] 25 mmol scale. [c] 10 mmol scale.

Open Access Article. Published on 24 September 2024. Downloaded on 1/21/2026 10:08:25 PM.
This article is licensed under a Creative Commons Attribution-NonCommercial 3.0 Unported Licence.

Table 2 Reaction optimisation in continuous flow mode

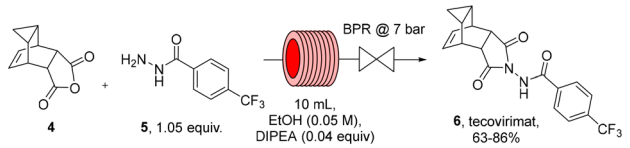

Entry	Temperature and time	Yield[a] of **6**	Remaining **5** [a]
1	110 °C, 15 min	77%	20%
2	120 °C, 15 min	85%	14%
3	130 °C, 15 min	73%	7%
4	120 °C, 20 min	63%	20%
5	125 °C, 15 min	67%	20%
6[b]	120 °C, 15 min	84%	14%
7[b,c]	120 °C, 15 min	86%[d]	—

[a] Determined by ^{1}H NMR of the crude reaction mixture using 1,3,5-trimethoxybenzene as an internal standard. [b] 0.1 M in ethanol. [c] 1 g scale. [d] Isolated yield.

Therefore, we wished to reductively desymmetrise **4** *via* a $NaBH_4$-mediated conversion of the anhydride moiety. As shown in Scheme 2, this transformation gave product **7** as a single diastereoisomer in a high yield of 74% along with the lactone structure **8**. The latter can be obtained as the major product (87% yield) when using an excess of the reducing agent. As both products are crystalline materials, single crystal X-ray diffraction was used to unambiguously confirm their structure.[17] Pleasingly, gram quantities of **7** could be accessed *via* this simple protocol which enabled further studies on this versatile scaffold.

Next, we evaluated the reactivity of compound **7** with different commercially available aryl hydrazine species. This showed that the corresponding condensation products **10** can be obtained in high chemical yields and as single isomers when treating **7** with the desired aryl hydrazine (as HCl salt, 1.5 equiv.) in the presence of triethylamine in refluxing methanol (Scheme 3). As shown below, the desired adducts are obtained in high yields within 1 hour. Amongst the hydrazine partners investigated only 2-fluorophenyl hydrazine showed a slightly different reactivity as a secondary adduct (**10d′**) was isolated as a minor component under these conditions.

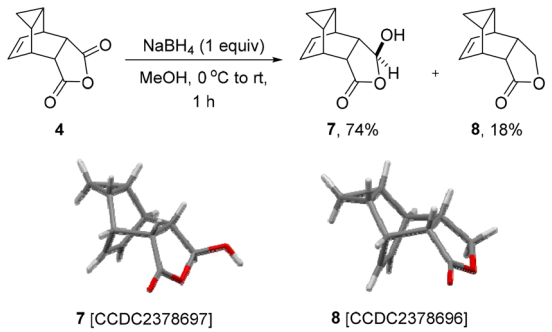

Scheme 2 Reductive desymmetrisation of **4** using $NaBH_4$ (X-ray structures are shown at the 50% probability level).

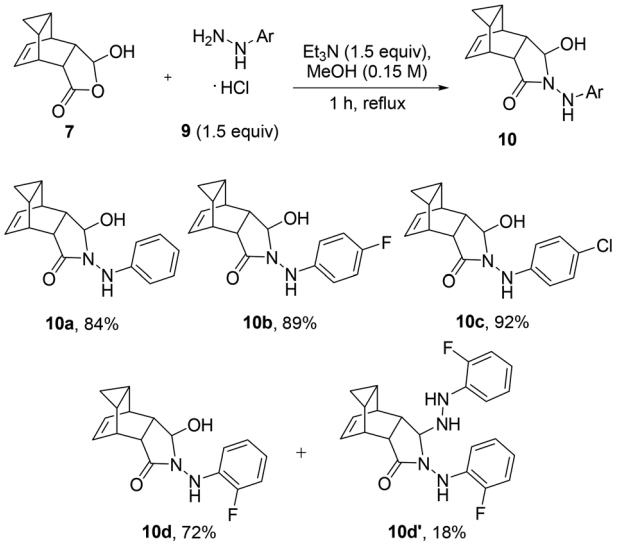

Scheme 3 Derivatisation studies between **7** and aryl hydrazine hydrochlorides.

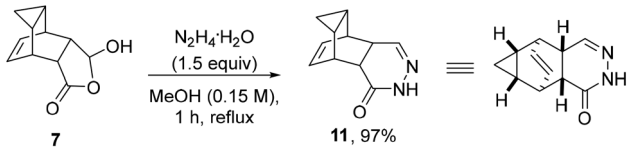

Scheme 4 Reaction between scaffold **7** and hydrazine hydrate.

Interestingly, a different product outcome was observed when subjecting scaffold **7** to analogous condensation conditions with hydrazine hydrate. As depicted in Scheme 4, a 6-membered ring product was obtained in 97% yield whereby two molecules of water were eliminated to give the embedded 4,5-dihydropyridazin-3(2*H*)-one ring system. These findings differ from the observations of Martin and coworkers[18] who reported that both 5- and 6-membered ring products can be formed when condensing hydrazine with simpler 5-hydroxydihydrofuran-2(3*H*)-ones. Given the different functionalities present, this unexpected outcome opens opportunities for further elaboration of the resulting heterocyclic product (**11**) to generate libraries of drug-like products.

Conclusions

In conclusion, we report an efficient 2-step continuous flow synthesis of the antiviral tecovirimat under high-temperature conditions. Reaction intensification thereby provides access to this API in 1 hour with an overall yield of 84%. Key to this success was the generation of a complex anhydride intermediate (**4**) with high productivity, which enabled further synthetic studies *via* a reductive desymmetrisation process. Condensation reactions of the resulting products with different hydrazines afforded additional heterocyclic scaffolds

Open Access Article. Published on 24 September 2024. Downloaded on 1/21/2026 10:08:25 PM.
This article is licensed under a Creative Commons Attribution-NonCommercial 3.0 Unported Licence.

in high chemical yields. These results demonstrate the value of flow-based reaction cascades for the streamlined generation of complex building blocks, that can find applications as medicinally relevant scaffolds.

Author contributions

A. B. conducted the experimental work, purified and characterised the reported products, and wrote the initial draft of this paper. M. B. supervised the project and edited the manuscript. A. B. and M. B. secured the funding and designed the research project.

Data availability

All data generated during this study are deposited in the ESI.† ^{1}H, ^{19}F and ^{13}C-NMR spectra for all reported compounds can be found in the ESI.†

Conflicts of interest

There are no conflicts to declare.

Acknowledgements

We are grateful to the Irish Research Council for providing a postgraduate scholarship (GOIPG/2020/1177, to A.B.). Dr Yannick Ortin and Dr Jimmy Muldoon are thanked for assistance with NMR and MS analysis (UCD). The authors are grateful to Dr Julia Bruno Colmenarez (UCD) for determining the X-ray structures reported in this work. Instrumentation support *via* the Comprehensive Molecular Analysis Platform (CMAP) initiative under the SFI Research Infrastructure Programme in 2019 (reference 18/RI/5702), and BiOrbic, the SFI Bioeconomy Research Centre (with the support of the School of Chemistry and UCD) and the UCD Equip Funding programme (2020 and 2022) is gratefully acknowledged. We wish to thank Science Foundation Ireland for supporting our research program through a Future Frontiers Project grant (20/FFP-P/8712). We thank Sarah Flynn (CEM Technology (Ireland) Ltd) for the loan of the microwave reactor used in this study.

References

1 (*a*) W. Wei, S. Cherukupalli, L. Jing, X. Liu and P. Zhan, *Drug Discovery Today*, 2020, **25**, 1839–1845; (*b*) D. C. Combo, K. Tallapragada, R. Jain, J. Chewning, A. A. Mazurov, J. D. Speake, T. A. Hauser and S. Toler, *J. Chem. Inf. Model.*, 2013, **53**, 327–342; (*c*) J. Meyers, M. Carter, N. Y. Mok and N. Brown, *Future Med. Chem.*, 2016, **8**, 1753–1767.

2 G. Calvo-Martín, D. Plano, N. Martínez-Sáez, C. Aydillo, E. Moreno, S. Espuelas and C. Sanmartín, *Pharmaceuticals*, 2022, **15**, 1465.

3 L. Wanka, K. Iqbal and P. R. Schreiner, *Chem. Rev.*, 2013, **113**, 3516–3604.

4 K. F. Biegasiewicz, J. R. Griffiths, G. P. Savage, J. Tsanaktsidis and R. Priefer, *Chem. Rev.*, 2015, **115**, 6719–6745.

5 (*a*) C. Hanna, *Toxicol. Appl. Pharmacol.*, 1960, **2**, 379–391; (*b*) Y. Zhang, T. W. Kensler, C. G. Cho, G. H. Posner and P. Talalay, *Proc. Natl. Acad. Sci. U. S. A.*, 1994, **91**, 3147–3150; (*c*) D. B. Calne and J. L. Reid, *Drugs*, 1972, **4**, 49–74; (*d*) J. D. Parkes, *Drugs*, 1981, **21**, 341–353; (*e*) R. Jackisch, H. Y. Huang, W. Reimann and N. Limberger, *J. Pharmacol. Exp. Ther.*, 1993, **264**, 889–898; (*f*) A. Kostelnik, A. Cegan and M. Pohanka, *BioMed Res. Int.*, 2017, **2017**, 2532764; (*g*) https://www.fda.gov/news-events/press-announcements/fda-approves-first-drug-indication-treatment-smallpox(accessed on August 1st, 2024).

6 J. Leitich and G. Sprintschnik, *Chem. Ber.*, 1986, **119**, 1640–1660.

7 (*a*) R. Jordan, T. R. Bailey, S. R. Rippin and D. Dai, *U.S. Pat*, US8530509B2, 2013; (*b*) R. Jordan, T. R. Bailey, S. R. Rippin and D. Dai, *U.S. Pat*, US8802714B2, 2014; (*c*) S. R. Tyavanagimatt, M. A. C. L. Stone, W. C. Weimers, D. Nelson, T. C. Bolken, D. E. Hruby, M. H. O'Neill, G. Sweetapple and K. A. McCloughan, *U.S. Pat*, US20110236434A1, 2011; (*d*) S. R. Tyavanagimatt, M. A. C. L. S. Anderson, W. C. Weimers, D. Nelson, T. C. Bolken, D. E. Hruby, M. H. O'Neill, G. Sweetapple and K. A. McCloughan, *U.S. Pat*, US20160107993A1, 2016; (*e*) S. R. Tyavanagimatt, M. A. C. L. S. Anderson, W. C. Weimers, D. Nelson, T. C. Bolken, D. E. Hruby, M. H. O'Neill, G. Sweetapple and K. A. McCloughan, *U.S. Pat*, US20180193308A1, 2018; (*f*) S. R. Tyavanagimatt, M. A. C. L. S. Anderson, W. C. Weimers, D. Nelson, T. C. Bolken, D. E. Hruby, M. H. O'Neill, G. Sweetapple and K. A. McCloughan, *U.S. Pat*, US20180311213A1, 2018; (*g*) S. R. Tyavanagimatt, M. A. C. L. S. Anderson, W. C. Weimers, D. Nelson, T. C. Bolken, D. E. Hruby, M. H. O'Neill, G. Sweetapple and K. A. McCloughan, *U.S. Pat*, US9744154B2, 2017, B2, 2018; (*h*) S. R. Tyavanagimatt, M. A. C. L. S. Anderson, W. C. Weimers, D. Nelson, T. C. Bolken, D. E. Hruby, M. H. O'Neill, G. Sweetapple and K. A. McCloughan, *U.S. Pat*, US10045964B2, 2018; (*i*) S. R. Tyavanagimatt, M. A. C. L. Stone, W. C. Weimers, D. Nelson, T. C. Bolken, D. E. Hruby, M. H. O'Neill, G. Sweetapple and K. A. McCloughan, *U.S. Pat*, US9339466B2, 2016; (*j*) M.-X. Dong, J. Zhang, X.-Q. Peng, H. Lu, L.-H. Yun, S. Jiang and Q. Dai, *Eur. J. Med. Chem.*, 2010, **45**, 4096–4103; (*k*) Q. Dai, M.-X. Dong and J. Hu, *Chin. Pat*, CN101445478A, 2009; (*l*) H. Wang, D. Zhang, Y. Dou, L. Xu, Y. Guo, Y. Sun, Z. Bei, Y. Yang, P. Dong, L. Li and L. Yang, *Chin. Pat*, CN101906064A, 2010; (*m*) R. F. Jordan and S. R. Rippin, WO2004112718A3, 2005; (*n*) D. L. Hughes, *Org. Process Res. Dev.*, 2019, **23**, 1298–1307.

 This journal is © The Royal Society of Chemistry 2024

Open Access Article. Published on 24 September 2024. Downloaded on 1/21/2026 10:08:25 PM.
This article is licensed under a Creative Commons Attribution-NonCommercial 3.0 Unported Licence.

8 E. M. Bonku, H. Qin, A. Odilov, F. Yang, X. Xing, X. Wang, S. D. Guma and J. Shen, *Org. Process Res. Dev.*, 2023, **27**(11), 1984–1991.

9 (*a*) K. Donnelly and M. Baumann, *Chem. Commun.*, 2021, **57**, 2871–2874; (*b*) A. Bonner and M. Baumann, *Org. Process Res. Dev.*, 2024, **28**, 1567–1575; (*c*) R. Crawford and M. Baumann, *Chem. – Eur. J.*, 2024, **30**, e202401491; (*d*) M. Smyth, T. S. Moody, S. Wharry and M. Baumann, *Synlett*, 2024, 285–290; (*e*) K. Donnelly and M. Baumann, *Chem. – Eur. J.*, 2024, **30**, e202400758.

10 (*a*) L. Buglioni, F. Raymenants, A. Slattery, S. D. A. Zondag and T. Noël, *Chem. Rev.*, 2022, **122**, 2752–2906; (*b*) T. Razzaq and C. O. Kappe, *Chem. – Asian J.*, 2010, **5**, 1274–1289; (*c*) M. Guidi, P. H. Seeberger and K. Gilmore, *Chem. Soc. Rev.*, 2020, **49**, 8910–8932; (*d*) M. Brzozowski, M. O'Brien, S. V. Ley and A. Polyzos, *Acc. Chem. Res.*, 2015, **48**, 349–362.

11 (*a*) C. R. Sagandira, S. Nqeketo, K. Mhlana, T. Sonti, S. Gaqa and P. Watts, *React. Chem. Eng.*, 2022, **7**, 214–244; (*b*) B. Gutmann, D. Cantillo and C. O. Kappe, *Angew. Chem., Int. Ed.*, 2015, **54**, 6688–6729; (*c*) R. Porta, M. Benaglia and A. Puglisi, *Org. Process Res. Dev.*, 2016, **20**, 2–25; (*d*) M. Baumann and I. R. Baxendale, *Beilstein J. Org. Chem.*, 2015, **11**, 1194–1219.

12 J. Britton and C. L. Raston, *Chem. Soc. Rev.*, 2017, **46**, 1250–1271.

13 (*a*) A. M. Kearney, S. G. Collins and A. R. Maguire, *React. Chem. Eng.*, 2024, **9**, 990–1013; (*b*) J. D. Williams, P. Sagmeister and C. O. Kappe, *Curr. Opin. Green Sustainable Chem.*, 2024, **47**, 100921.

14 (*a*) J. García-Lacuna and M. Baumann, *Beilstein J. Org. Chem.*, 2022, **18**, 1720–1740.

15 J. Blümel and F. H. Köhler, *Chem. Ber.*, 1993, **126**, 1283–1290.

16 M. M. Efremova, A. P. Molchanov, A. S. Novikov, G. L. Starova, A. A. Muryleva, A. V. Slita and V. V. Zarubaev, *Tetrahedron*, 2020, **76**, 131104.

17 CCDC 2378696 and 2378697† contain the supplementary crystallographic data for this paper (**https://www.ccdc.cam.ac.uk/structures**).

18 (*a*) F. Delgado, M. R. Martin and M. V. Martin, *Tetrahedron*, 2001, **57**, 4389–4395; (*b*) L. Somogyi, *Liebigs Ann. Chem.*, 1985, **1985**, 1679–1691; (*c*) J. E. Francis, K. J. Doebel, P. M. Schutte, E. F. Bachmann and R. E. Detlefsen, *Can. J. Chem.*, 1982, **60**, 1214–1232.